

# Detecting Anomalies in Measured Thermal Neutron Flux Profiles of SAFARI-1 Research Reactor

Rethabile Kgolobe<sup>1</sup>, Pavel M. Bokov<sup>2</sup>, Simon H. Connell<sup>1</sup>, Charis Harley<sup>1</sup>, Bongani G. Maqabuka<sup>1</sup>, Lesego E. Moloko<sup>2</sup>, Rian H. Prinsloo<sup>2</sup>

<sup>1</sup>University of Johannesburg

<sup>2</sup>Necsa



# Introduction

---

# Background

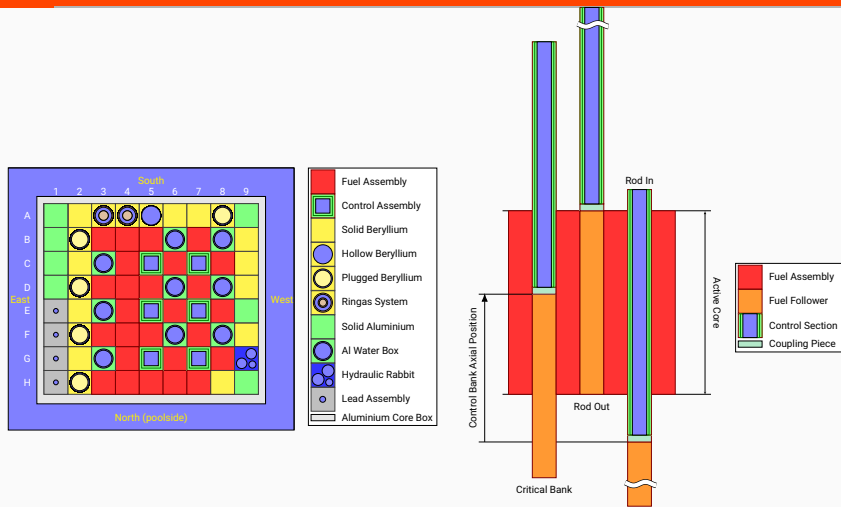


**Figure 1:** SAFARI-1 layout left (top view) and right (side view) [3].

- Accurate neutron flux measurement is vital for reactor safety and performance optimization [4].
- SAFARI-1 is a 20 MW pool-type reactor in an  $8 \times 9$  grid, with 26 fuel and 6 control elements and other components such as beryllium, etc [1].

# Copper Wire Measurement

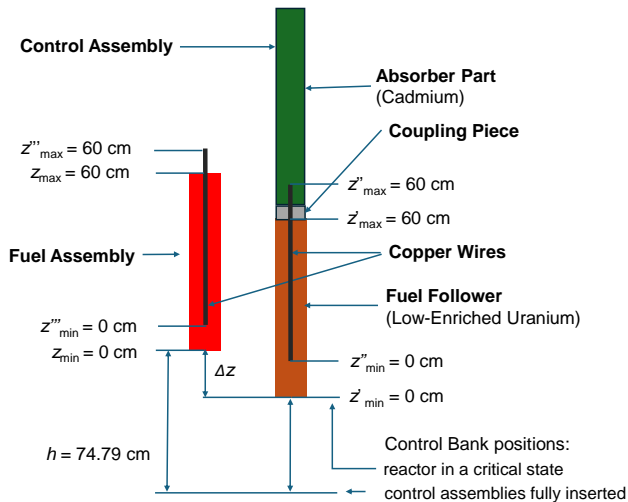


**Figure 2:** Side view of fuel and control rod configuration

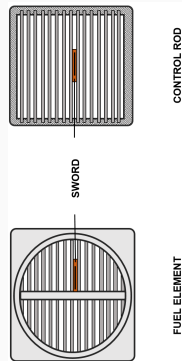


**Figure 3:** Top view of fuel and control rod layout.

- Neutron flux profiles measured using natural copper wires at each cycle start
- Incomplete insertion of the copper wire can cause shifts in axial measurements, leading to anomalies [2].

# Study Objective

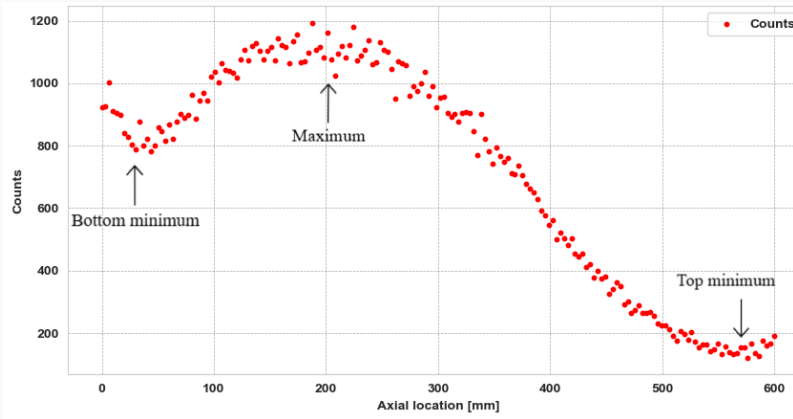


**Figure 4:** Illustration flux distribution with three key features.

- Assess which key features are more stable for estimating axially shifted measurements.
- Evaluate sensitivity of key profile features to control rod movement:
  - **Bottom Minimum**
  - **Peak Maximum**
  - **Top Minimum**

# Methodology

---

## Research Approach

1. **Data Preprocessing** – Clean and structure neutron flux data.
2. **Visualization** – 1D/2D/3D plots of axial flux distribution.
3. **Polynomial Fitting** – Extract features from flux profiles.
4. **Statistical Analysis** – Standard deviation, MAD, Spearman correlation, etc. of key flux features.
5. **Hypothesis Testing** – Perform  $\chi^2$  Goodness-of-Fit tests to evaluate significance and accept or reject  $H_0$  at 95% confidence of key feature vs. control rod positions.

## Results

---



# Raw Experimental Counts and Control Rod

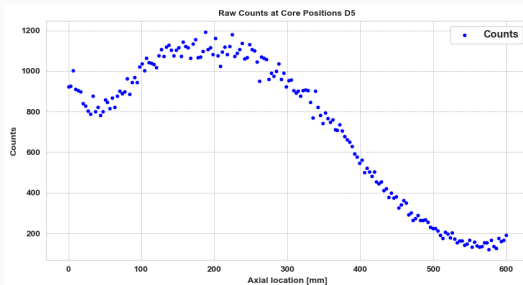


**Figure 5:** Fuel Assembly.

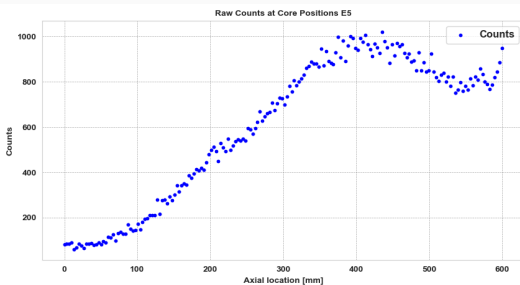


**Figure 6:** Control Assembly.

# Decay Correction

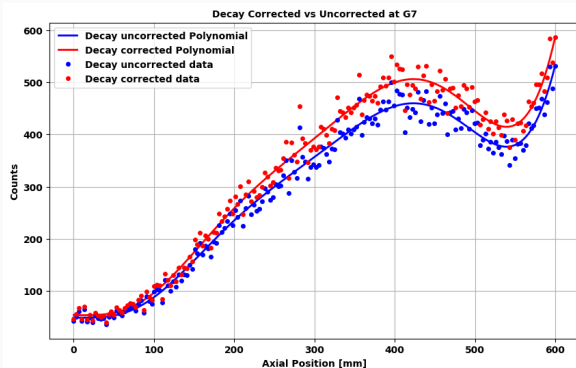
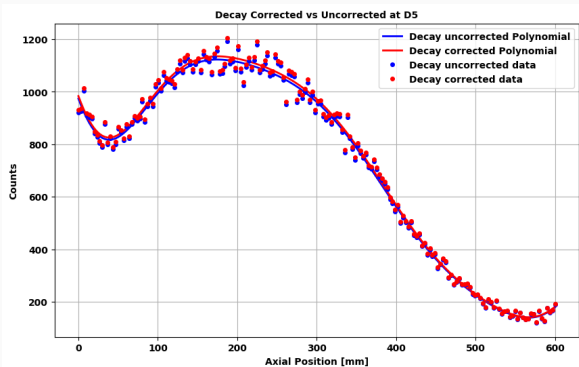


**Figure 7:** Comparison of raw counts and decay-corrected measurement, fuel element (left) and control rod (right).

## 2D Flux Visualization

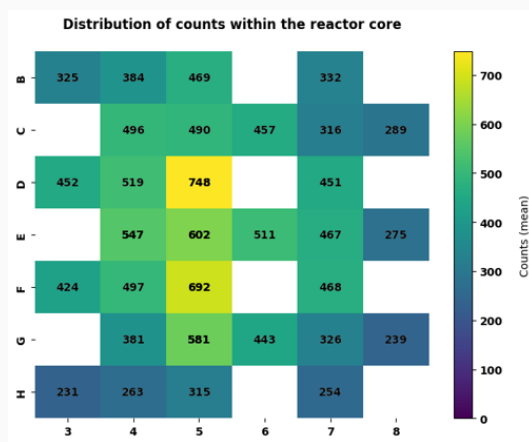
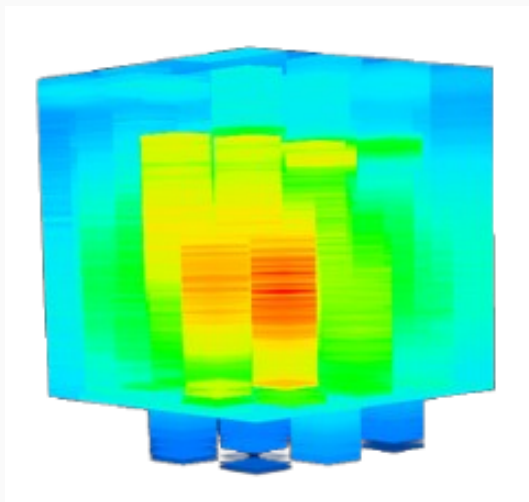


Figure 8: Axial distribution (2D) of neutron flux counts

## 3D Reactor Core



**Figure 9:** 3D flux distribution visualization of reactor core positions.

# Polynomial Fitting and Key Feature Extraction

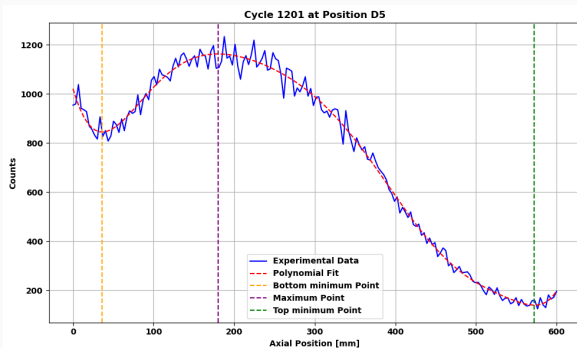
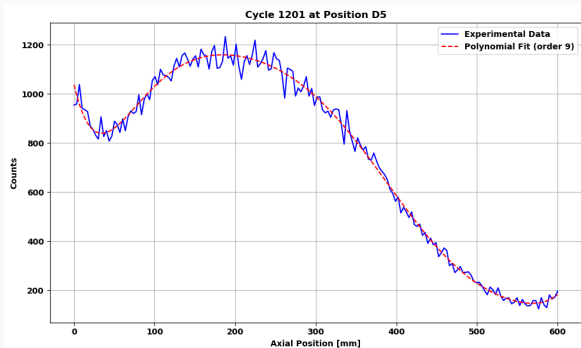


**Figure 10:** Left: Polynomial smoothing of the experimental flux profile. Right: Extraction of key axial features (minima and maxima) from the fitted curve.

# Control Bank Position Effect

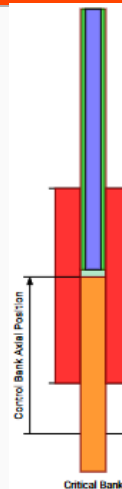
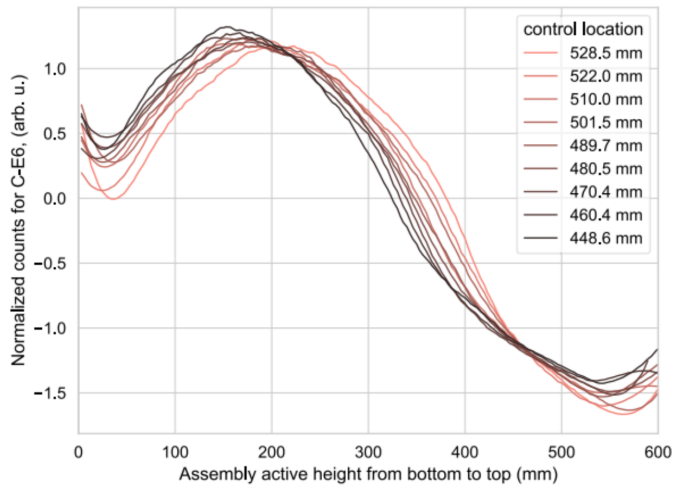


**Figure 11:** Effect of control bank position on neutron flux profile (left) with visual representation of control rod insertion (right).

# Bottom Minimum vs. Bank Position

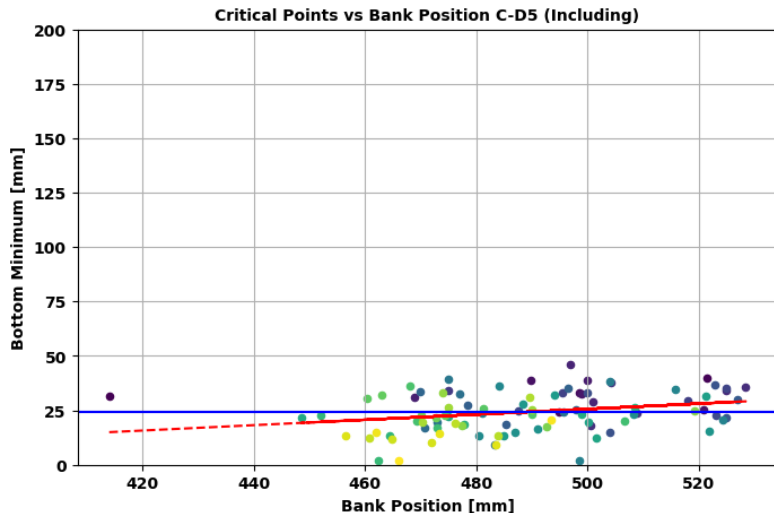
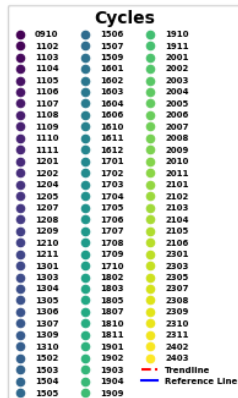
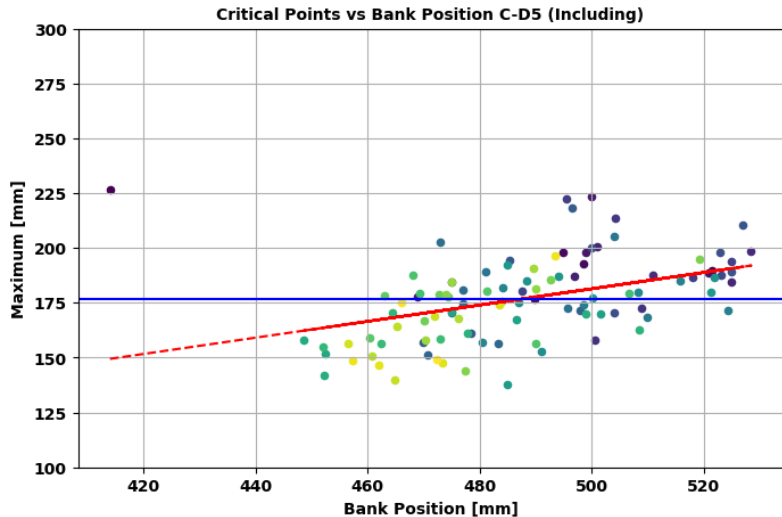


Figure 12: Bottom minimum location over bank positions with corresponding legend (right).

# Peak Maximum vs. Bank Position



**Figure 13:** Peak location vs. control rod position with corresponding legend (right).



# Top Minimum vs. Bank Position

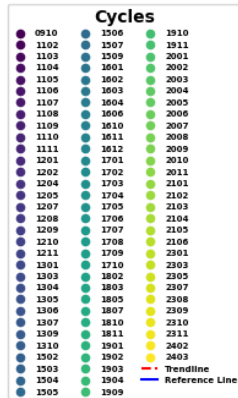
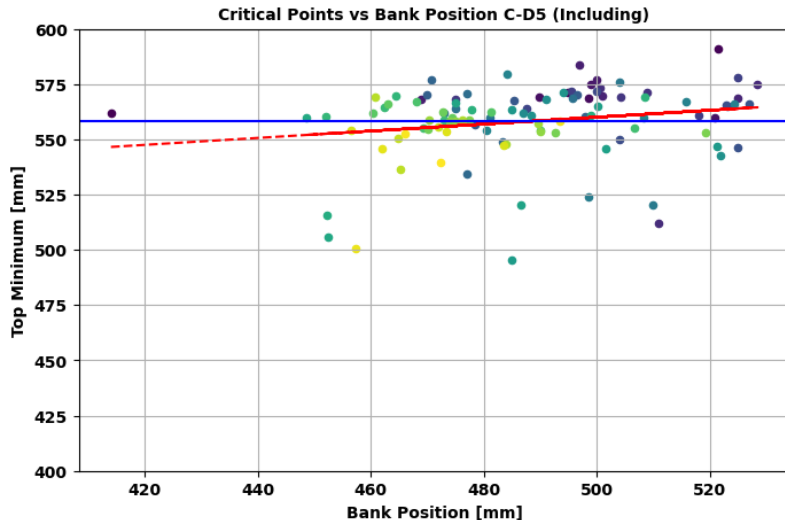


Figure 14: Top minimum vs. bank positions with corresponding legend (right).

## Feature Sensitivity Analysis

- **Peak Maximum** showed the highest correlation with control rod movement at C-D5 (Spearman = 0.54), confirming sensitivity to rod position.
- **Bottom Minimum** had a moderate correlation (Spearman 0.33).
- **Top Minimum** showed the lowest correlation at C-D5 (Spearman = 0.24), suggesting it is least affected by rod movement and thus most stable.
- At C-H3, **Top Minimum** still maintained lower correlations, reinforcing its reliability for identifying axial shifts.

## Minuit Quadratic Fitting - Bottom Minimum

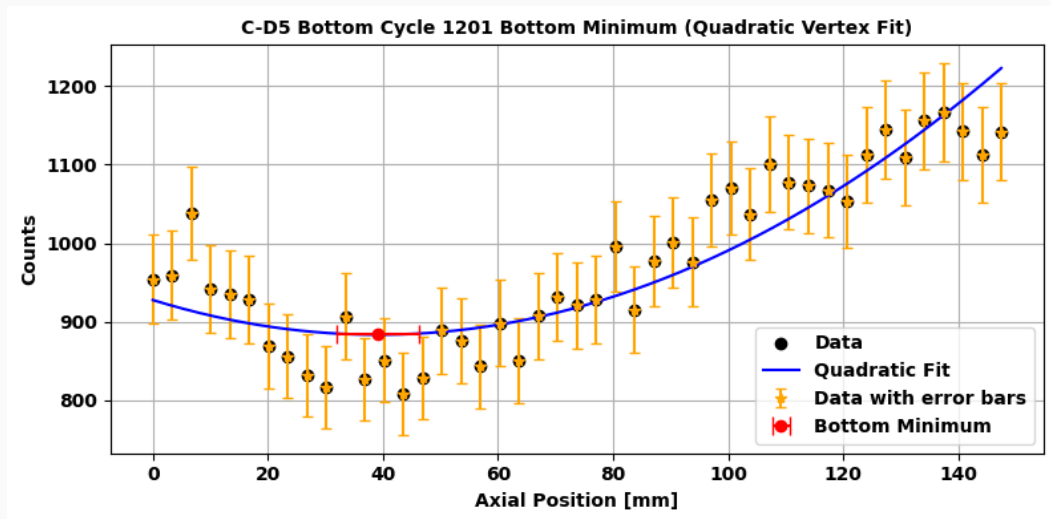


Figure 15: Quadratic vertex fitting for bottom minimum feature.

## Minuit Quadratic Fitting - Peak Maximum

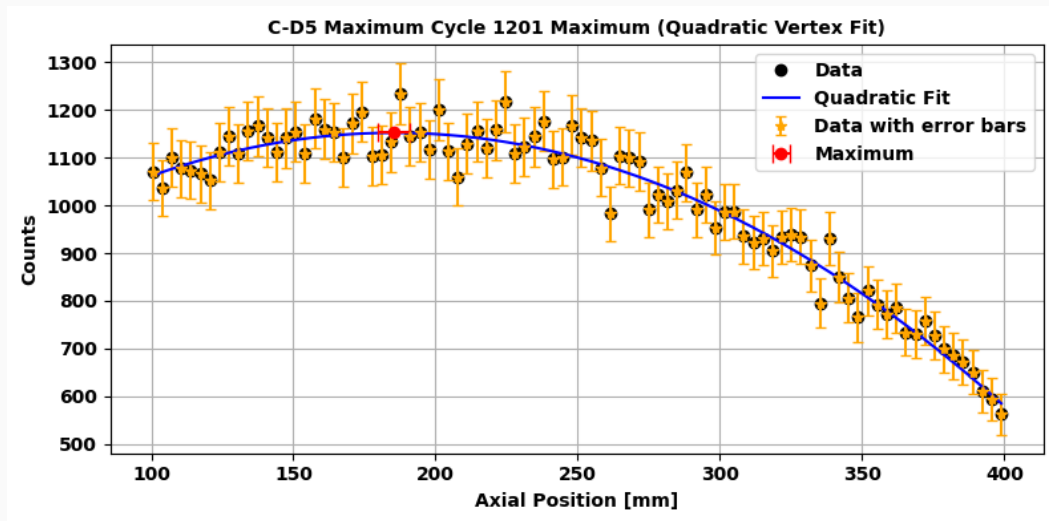


Figure 16: Quadratic vertex fitting for peak maximum feature.

## Minuit Quadratic Fitting - Top Minimum

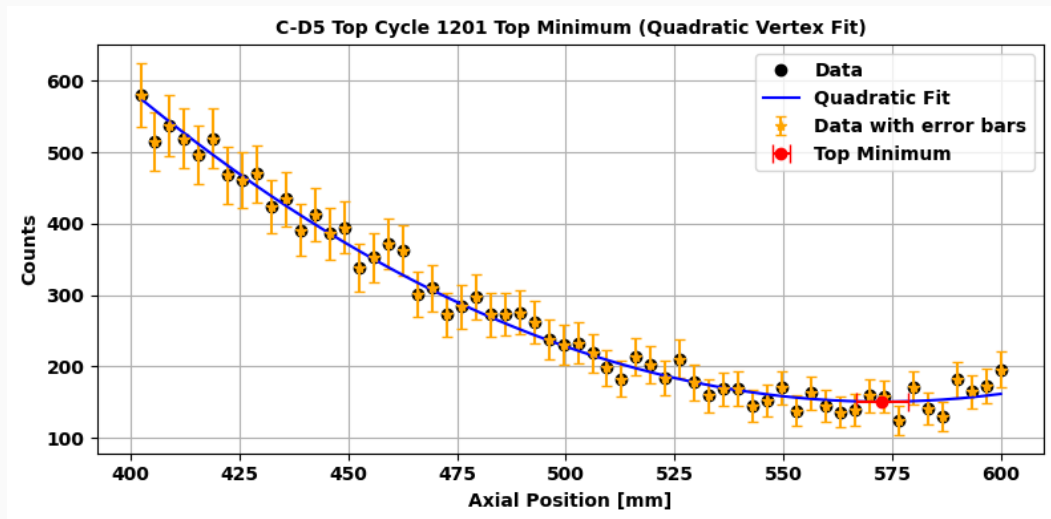


Figure 17: Quadratic vertex fitting for top minimum feature.

## Effect of Scaling Errors by Factor 1.5

Cycle	Region	Poly-fit	Taylor	Cov. Err	Profile Err	Red. $\chi^2$ (Init)	Red. $\chi^2$ (Scaled)
0910	Bottom min	31.76	39.71	1.91	2.93	2.03	0.90
0910	Maximum	226.71	218.93	2.31	3.48	0.93	0.42
0910	Top min	562.06	561.86	2.68	4.03	1.64	0.73
1102	Bottom min	39.65	49.67	0.98	1.48	1.83	0.81
1102	Maximum	189.74	194.63	2.33	3.51	0.78	0.35
1102	Top min	590.81	600.00	1.90	1.61	1.14	0.51
1103	Bottom min	24.47	23.41	5.31	8.59	1.24	0.55
1103	Maximum	197.85	194.30	2.39	3.58	1.14	0.51
1103	Top min	571.11	580.81	8.15	6.87	1.21	0.54

# Hypothesis Testing Results - Bottom Minimum

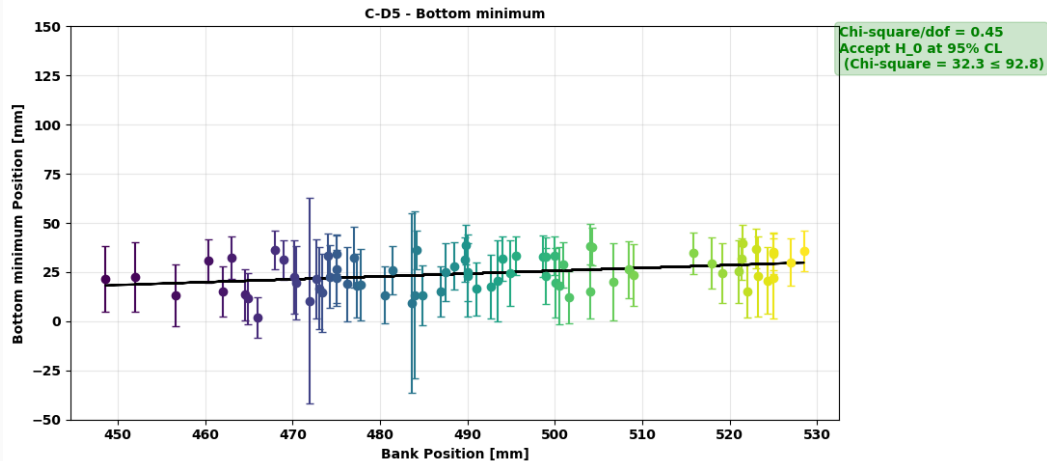


Figure 18: Hypothesis Testing.

# Hypothesis Testing Results - Peak Maximum

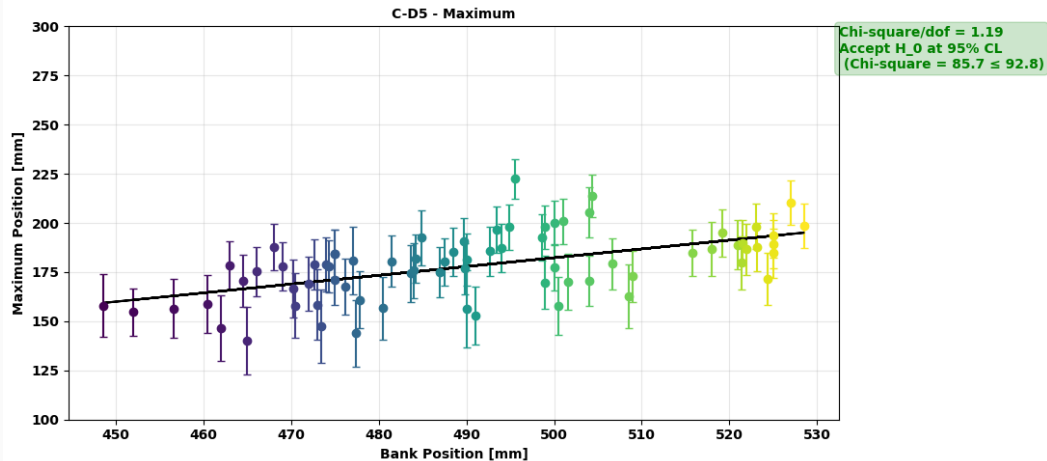


Figure 19: Hypothesis Testing.



# Hypothesis Testing Results - Top Minimum

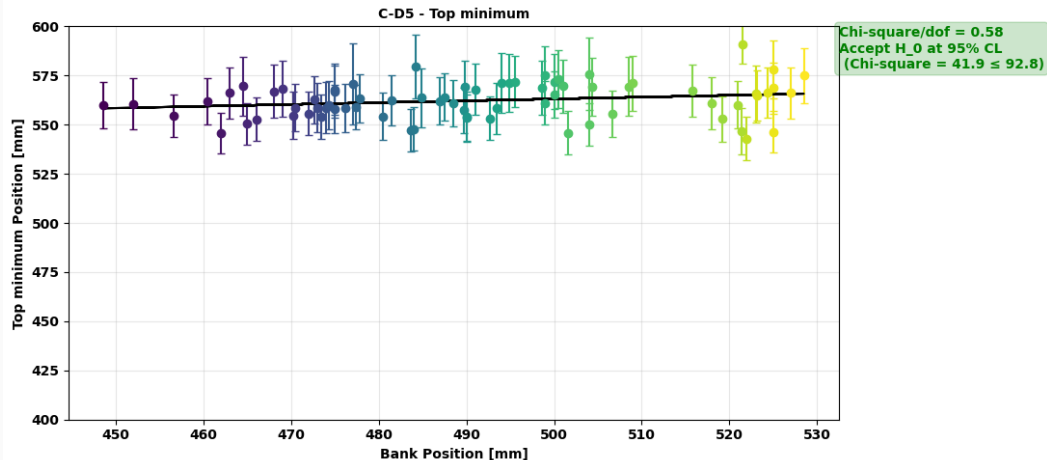


Figure 20: Hypothesis Testing.

## Chi-Square Test Results for Position C-D5 ( $\alpha = 8$ )

Position	Region	DOF	$\chi^2$	$\chi^2_{\text{critical}}$	$\chi^2_{\text{reduced}}$	Slope	$H_0$ at $\approx 95\%$
C-D5	Bottom minimum	72	32.33	92.81	0.449	0.1448	Accepted
	Maximum	72	85.67	92.81	1.190	0.4467	Accepted
	Top minimum	72	41.87	92.81	0.582	0.0931	Accepted

# Results

- **Peak Maximum:** Most sensitive to control rod position (Spearman = 0.54 at C-D5).
- **Top Minimum:** Least sensitive across cycles (Spearman = 0.24), most stable.
- **Bottom Minimum:** Moderately sensitive and more affected by noise.
- **Model Fit:** Reduced  $\chi^2 < 1.2$  for all features; improved further with error scaling.
- **H<sub>0</sub> Testing:** Accepted at 95% confidence, all features fit expected behavior.

- This work contributes a method for detecting axial anomalies in SAFARI-1, among others being explored.
- **Top Minimum** is the most reliable for identifying misalignments based on the statistical results.
- No significant deviations found (95% confidence), validating feature stability and fitting approach.

# Acknowledgment

---



# Acknowledgment

- Lesedi Nuclear Services.
- Necsa for additional data.
- RC Group.

**Thank You!**

-  L. E. Moloko, P. M. Bokov, Wu X., and Ivanov K. N.  
**Quantification of neural networks uncertainties with applications to SAFARI-1 axial neutron flux profiles.**  
*In Proceedings of the International Conference on Physics of Reactors (PHYSOR 2022), ANS, Pittsburgh, Pennsylvania, USA, pages 1398–1407, 2022.*
-  LE Moloko, PM Bokov, and KN Ivanov.  
**Estimation of the axial neutron flux profiles in the SAFARI-1 core using artificial neural networks.**  
*In Proceedings of the 2021 International Conference on Mathematics and Computational Methods Applied to Nuclear Science and Engineering (M&C-2021), Raleigh, North Carolina, pages 1644–1653, 2021.*



-  Lesego E Moloko, Pavel M Bokov, Xu Wu, and Kostadin N Ivanov.  
**Prediction and uncertainty quantification of safari-1 axial neutron flux profiles with neural networks.**  
*Annals of Nuclear Energy*, 188:109813, 2023.
-  L Snoj, A Trkov, R Jaćimović, P Rogan, G Žerovnik, and M Ravnik.  
**Analysis of neutron flux distribution for the validation of computational methods for the optimization of research reactor utilization.**  
*Applied Radiation and Isotopes*, 69(1):136–141, 2011.